Spring 2017

Effects of the microenvironment surrounding Cys433 in *Arabidopsis* β-amylase-1 and -3 on the sensitivity to glutathionylation by nitrosoglutathione

Matthew R. Kohler
James Madison University

Effects of the microenvironment surrounding Cys433 in *Arabidopsis* β-amylase-1 and -3 on the sensitivity to glutathionylation by nitrosoglutathione

An Honors College Project Presented to

the Faculty of the Undergraduate

College of Science and Mathematics

James Madison University

by Matthew Russell Kohler

May 2017

Accepted by the faculty of the Department of Biology, James Madison University, in partial fulfillment of the requirements for the Honors College.

FACULTY COMMITTEE:

Project Advisor: Jonathan Monroe, Ph.D.
Professor, Biology

Reader: Christopher Berndsen, Ph.D.
Assistant Professor, Chemistry and Biochemistry

Reader: Kimberly Slekar, Ph.D.
Associate Professor, Biology

HONORS COLLEGE APPROVAL:

Bradley R. Newcomer, Ph.D.,
Dean, Honors College

PUBLIC PRESENTATION

This work is accepted for presentation, in part or in full, at Biosymposium on April 21, 2017

Table of Contents

List of Tables and Figures

Tables

Figures

Acknowledgements

I would like to first thank my advisor Dr. Monroe for helping me throughout my undergraduate research experience. He brought me into lab and guided me endlessly from learning how to think and write like a scientist to showing me how to be a good teacher. I also cannot thank Dr. Storm enough for patiently answering all of my questions and helping me throughout my time in the lab. The mentoring from Dr. Monroe and Dr. Storm has made my research experience the most important academic experience I had at JMU. I would also like to thank the other lab members for getting up early to help me with assays, offering an extra hand, and making my lab experience so enjoyable. Thank you to my readers, Dr. Berndsen and Dr. Slekar, for providing feedback on my thesis. A special thanks goes to Dr. Berndsen for giving me a foundation in biochemistry and teaching me about pKas, which was the spark for one of the main ideas behind this thesis. Finally, I would like to thank the National Science Foundation for funding this research.

Abstract

Glutathionylation is a reversible post-translational modification of proteins involving the transfer of glutathione to the thiols of specific cysteine residues. While the mechanism behind glutathionylation is known, the specificity of cysteine glutathionylation is not understood. It is known, however, that the two main factors affecting the susceptibility to glutathionylation are the reactivity and accessibility of cysteines in proteins, which is determined by the microenvironment. Using β-amylases (BAMs) 1 and 3 from *Arabidopsis thaliana*, which have different sensitivities to nitrosoglutathione (GSNO), as a model, I attempted to provide insight into why some cysteines are glutathionylated by GSNO and others are not. Our lab found that GSNO inhibits BAM3 activity by glutathionylating Cys433 *in vitro*, yet BAM1 is unaffected by GSNO despite containing a cysteine at the same position. At a physiological level, the glutathionylation of BAM3 by GSNO may be important as BAM3 may be inhibited by a NO-induced modification under cold stress. Different microenvironments surrounding Cys433 in BAM1 and BAM3 could explain the different sensitivities these enzymes have to GSNO. I compared sequence alignments of BAM1 and BAM3 from a variety of flowering plants. If a position is important in making Cys433 in BAM3 and BAM1 sensitive and insensitive, respectively, to GSNO, then that position would likely be conserved within each BAM1 and BAM3 orthologous set but be different between the sets. After comparing sequence alignments and locating these positions in homology models, I hypothesized that H^{430}, N^{432}, and S^{434} might contribute to the sensitivity of Cys433 in BAM3 to GSNO, and that the corresponding amino acids in BAM1, D^{430}, L^{432}, and A^{434}, might contribute to its insensitivity. To test this hypothesis, I made three BAM3 mutants with the amino acid substitution H430D, N432L, or S434A and the corresponding BAM1 mutants, D430H, L432N, and A434S. All of the BAM1 mutants were

active but only the BAM3 mutant with the H430D substitution was active. I then treated the active mutants with GSNO and compared their sensitivity to the BAM3 and BAM1 controls. The BAM1-D430H and BAM1-A434S mutants were inhibited by 45% and 20%, respectively, by GSNO whereas the WT BAM1 control was insensitive to GSNO. The active BAM3 mutant, however, was just as sensitive to GSNO as the BAM3 control. Therefore, D^{430} and A^{434} may contribute to the insensitivity of Cys433 to glutathionylation by GSNO in BAM1. D^{430} may play a larger role in making Cys433 insensitive to GSNO in BAM1 than A^{434} because it is negatively charged, which could decrease the reactivity and/or the accessibility of Cys433.

Introduction

During the day, plants make sugar via photosynthesis, and about half of the sugar is used for energy production and biosynthesis (Smith and Stitt 2007). The other half, stored in chloroplasts as transitory starch, can then be mobilized at night to maintain cellular functions when photosynthesis is not occurring (Zeeman et al. 2010). The starch degradation pathway has been recently elucidated to involve multiple enzymes, but the mechanisms of regulation are not well characterized (Graf et al. 2010; Santelia et al. 2015).

Starch is an insoluble, crystalline polymer of glucose that is stored in plastids as granules. To hydrate the starch granules and allow amylolytic enzymes to access them, water dikinase phosphorylates the outer glucose residues of starch. Then, a series of debranching enzymes and phosphoglucan phosphatases linearize the glucan chains (Zeeman et al. 2004). Simultaneously, hydrolysis of linear glucans by β-amylases (BAMs) releases maltose (Zeeman et al. 2007), which is then exported to and metabolized in the cytosol (Niittyla et al. 2004).

Arabidopsis thaliana (Arabidopsis) has a gene family that encodes nine BAM-like proteins. Among the catalytically active BAMs, BAM1, -2, -3, and -6 are plastidic (Fulton et al. 2008; Li et al. 2009) while BAM5 is cytosolic (Wang et al. 1995). BAM1 and -3 are considered to be the predominant β-amylases involved in starch degradation in younger leaves (Fulton et al. 2008; Monroe et al. 2014). BAM2 and -6 may play a role in the breakdown of starch in older plants, but they do not contribute significantly to β-amylase activity in young leaves (Monroe et al. 2014). Among the catalytically inactive BAMs, BAM7 and -8 are targeted to the nucleus and function as transcription factors (Reinhold et al. 2011) whereas BAM4 and -9 are plastidic and have unknown regulatory roles (Fulton et al. 2008; Li et al. 2009).

While both BAM1 and -3 have important roles in transitory starch degradation in young leaves, they exhibit different cell-type specificities and optimum conditions (Monroe et al. 2014; Horrer et al. 2016). BAM3 is active during the night in mesophyll cells when temperatures and stromal pH are usually lower. Conversely, BAM1 is found in the guard cells of younger leaves and is active during the day when temperatures are usually higher and stromal pH is high. Consistent with these locations, BAM1 has an optimal activity at higher temperatures and is more active at a high pH compared to BAM3 (Monroe et al. 2014).

Not only are the optimal conditions of BAM3 and BAM1 different but also their roles in plants. While BAM3 contributes to the typical dynamics of starch degradation in which starch is synthesized during the day and broken down at night, BAM1 is a major player in guard cell starch mobilization (Horrer et al. 2016). In guard cells, starch is sustained throughout the night and is almost completely mobilized within the first 30 minutes of light. The resulting maltose produced by BAM1 in guard cells helps to increase the cell's osmolarity and therefore contributes to the regulation of stomatal opening (Santelia et al. 2015).

Due to the different cell-type specificities and roles of the BAM1 and -3 isozymes, it is not surprising that their regulation in response to cold stress is also different. Transcription of *BAM3* is induced by cold stress (Kaplan and Guy 2004), which could result in more BAM3 protein and, therefore, starch breakdown. However, Monroe et al. (2014) found that β-amylase activity and starch degradation decreases under cold stress, leading to starch accumulation. To identify the β-amylases involved, they made a series of Arabidopsis BAM knockout mutants using T-DNA insertion lines from the Arabidopsis Biological Resource Center. Arabidopsis mutants lacking all active BAMs except BAM3 (*bam516*) had lower β-amylase activity when exposed to 4°C for 4 days, which was similar to the decrease in β-amylase activity observed in

cold-stressed wild-type (WT) plants (our unpublished results). The β-amylase activity in mutant plants lacking all active BAMs except BAM1 (*bam536*) was unaffected by the same conditions. These results suggest that the decreased β-amylase activity observed in leaves under cold stress can be attributed to a decrease in BAM3 activity despite its high mRNA levels because the β-amylase activity of mutant plants lacking BAM3 was not affected by cold stress. A possible mechanism to explain these results is that BAM3 is inhibited by post-translational modification (PTM) under cold stress. Accumulating *BAM3* mRNA during cold stress may be advantageous because once the cold stress abates, the supply of *BAM3* could be rapidly translated into thermally-adapted β-amylase protein that could resume starch degradation (Monroe et al. 2014). The modification of BAM3 could therefore regulate starch degradation in response to stress.

Nitric oxide (NO) is a signaling molecule that is produced in plants exposed to various stresses (Bajguz 2014). While NO is quite unstable, it can combine with the tripeptide glutathione (GSH) to form nitrosoglutathione (GSNO). GSNO is an important molecule during the response of plants to biotic and abiotic stress (Corpas et al. 2013), and can serve as a mobile NO reservoir (Leterrier et al. 2011). Also, modification of proteins by GSNO can result in dynamic post-translational regulation of many metabolic proteins (Dalle-Donne et al. 2007). The two modifications caused by GSNO are nitrosylation, which involves transferring a nitrosyl group to cysteine thiols, and glutathionylation. Glutathionylation results in the formation of a disulfide bond between the thiol of GSH and the thiol of specific cysteines in proteins (Santelia et al. 2015). This is important as a reversible, and therefore protective, oxidation reaction (Gallogly and Mieyal 2007). Under oxidative conditions, reactive cysteines in proteins can become irreversibly oxidized to sulfinic and sulfonic acids (Paulsen and Carroll 2013). However, glutathionylation can serve as a protecting group and prevent irreversible oxidation (Grek et al

2013; Popov 2014). Interestingly, our lab has found that *in vitro,* GSNO inhibited the activity of purified BAM3 by over 80% within a few minutes of exposure but had almost no effect on pure BAM1, suggesting that GSNO can also serve as an inhibitor of BAM3 activity *in vitro*. GSNO-modified BAM3 was then treated with dithiothreitol (DTT), which reverses both nitrosylation and glutathionylation, or ascorbic acid, which only reverses nitrosylation, to determine whether nitrosylation or glutathionylation caused the inhibition of BAM3 *in vitro*. BAM3 activity recovered after DTT treatment but was unaffected after ascorbic acid treatment. Furthermore, after exposure to GSNO, BAM3 interacted with anti-GSH antibodies, indicating glutathionylation as the mechanism of GSNO modification.

To determine which cysteine residue(s) were glutathionylated in BAM3, our lab made a series of BAM3 mutants replacing one or more cysteines with non-cysteine amino acids and tested how sensitive each one was to GSNO. When C^{433} in BAM3 was replaced with serine, the mutant (C433S) was only inhibited by 10% after GSNO treatment as opposed to the 80% inhibition seen with the WT BAM3. Moreover, GSNO-treated BAM3-C433S did not show the glutathionylation band apparent in western blots of WT BAM3 probed with anti-GSH antibodies. After an analysis of the location of C^{433} within a homology model of BAM3, it was clear that glutathionylation of C^{433} could inhibit activity by interfering with starch binding as C^{433} is located on a loop near the active site. To determine if replacing more than one cysteine to non-cysteine residues decreased the sensitivity of BAM3 to GSNO, double cysteine substitution mutants were made. Even though the BAM3-C433S mutant was the only single mutant that became less sensitive to GSNO, a C177V/C257A double mutant was less sensitive to GSNO than the C177V and C257A single mutants. There were no glutathionylation bands in the

western blot of the BAM3-C433S, indicating that C^{177} and C^{257} are not glutathionylated, but they may influence the ability of C^{433} to become glutathionylated (Storm et al. unpublished).

Due to its insensitivity, BAM1 was expected to contain non-Cys residues at positions 177, 257, and 433 (numbering based on BAM3). This was the case at positions 177 and 257 in which BAM1 contains a Val and Ala, respectively. However, there is a Cys at position 433 in BAM1. Either that position is not glutathionylated in BAM1 or its glutathionylation does not affect activity. Based on the homology model of BAM1, though, C^{433} glutathionylation should still interfere with starch binding. The apparent insensitivity of BAM1 indicates that the microenvironment of C^{433} in BAM1 may be different than that of C^{433} in BAM3, resulting in differential sensitivity to glutathionylation.

Susceptibility of cysteines to redox modification, of which glutathionylation is one type, is determined mostly by the reactivity of the Cys residue and the accessibility of its thiol to the solvent (Dalle-Donnet et al. 2007). Common to all of the cysteine modifications is that ionization of the thiol side chain into the thiolate anion is a prerequisite for reactivity (Ferrer-Sueta et al. 2011). The pKa, the pH at which the concentration of the protonated state is equal to the deprotonated state, determines cysteine reactivity (Madzelan et al. 2012). The pKa of a protonatable group can change depending on the surrounding environment, and low pKa cysteine side chains are more likely to be in the deprotonated thiolate anion state and, therefore, more easily glutathionylated (Grek et al. 2013). Donation of hydrogen bonds to the cysteine side chain and electrostatic stabilization from nearby cationic residues are thought to be the main mechanisms for lowering the pKa of a thiol (Roos et al. 2012; Shekhter et al. 2010). These cationic residues that establish a basic microenvironment and may contribute to a lowered cysteine pKa include histidine, asparagine, and lysine. In addition, the peptide bonds in the

protein backbone have a dipole moment that is amplified in an α-helix (Miranda 2003). This α-helix macrodipole results in a partial positive charge at the N-terminal peptide bonds of the α-helix that can donate a hydrogen bond to a thiolate. Conversely, a hydrophobic microenvironment or anionic groups that cannot donate a hydrogen bond do not favor the thiolate form and render a cysteine less reactive.

Accessibility of a cysteine thiol to the solvent is another factor that contributes to the specificity of glutathionylation (Ghezzi et al. 2006). Largely determined by solvent exposure, accessibility is a function of the steric hindrance and physical location of a cysteine residue. Cysteines buried within a protein are much less likely to be modified because molecules in the solvent cannot interact with buried residues as easily. The charges of amino acids surrounding a cysteine may also influence the orientation of an approaching GSNO molecule, which has a net negative charge (Hye-Won et al. 2001). Overall, cysteine reactivity and accessibility are aspects of the microenvironment that may help to explain the biochemical reasons for the sensitivity and insensitivity of BAM3 and -1, respectively, to GSNO.

The objective of this study was to test the hypothesis that the microenvironment of C^{433} in BAM3 makes it susceptible to glutathionylation by GSNO whereas that of C^{433} in BAM1 makes it insensitive to GSNO. I sought to identify residues near C^{433} in BAM1 and BAM3 that are different, and then swap them using mutagenesis in order to determine if sensitivity to GSNO was affected.

The implication of this work is based on the gap in the literature about cysteine glutathionylation, which, along with other forms of redox regulation, has important but elusive roles in starch degradation (Santeli et al. 2015). More generally, this research may be able to contribute useful information in order to predict glutathionylation sites since the factors

contributing to the specificity of glutathionylation are not well characterized (Dalle-Donne et al. 2007). Currently, there is a program called GSHsite that predicts the sensitivity of glutathionylation using only the 10 amino acids before and after a cysteine residue in a protein's primary structure. While GSHsite bases its predictions using experimentally identified glutathionylation sites in mouse macrophages, it does not account for the microenvironment around those sites, which can alter the reactivity of cysteines and the accessibility of their thiols to the solvent. We have a unique opportunity in working with a cysteine residue that is not involved in the mechanism of catalysis yet its glutathionylation has a profound effect on activity. The importance is that we can modify amino acids around C^{433} without significantly disturbing the catalytic activity of BAM1 and -3 as opposed to working with an enzyme in which mutants are catalytically inactive (Zaffafnini et al. 2016; Madzelan et al. 2012; Miranda 2002). I hope to help bridge the gap in our understanding of GSNO and starch metabolism as well as contribute information to develop more comprehensive prediction sites as databases try to incorporate a more structure-based approach to predict redox-sensitive cysteine residues (Marino and Gladyshev 2009).

Methods

Plant Growth Conditions

Arabidopsis thaliana (Arabidopsis) ecotype Columbia (Col-0) plants were grown at 22°C with a 12 hour light / 12 hour dark photoperiod and 130 µmol m^{-2} s^{-1} illumination. Each 5'' pot contained Sunshine Mix#3 (Sun Gro Horticulture) with 5 plants (Monroe et al. 2014). Transfer DNA (T-DNA) lines, obtained from the Arabidopsis Biological Resource Center (ABRC), included *bam1* (Salk_004259), *bam3* (Salk 041214), *bam5* (Salk_004259), and *bam6* (Salk_023637). Triple mutant plants were generated by crossing homozygous T-DNA mutant plants and confirming with PCR by others in the lab. For SNP experiments, the triple mutant *bam516* and *bam536* plants were grown in normal growth conditions and sprayed with 2 mM SNP or water (control). After 5 hours, the leaves were harvested and frozen at -80°C before analysis.

β-Amylase Activity Assays

For assays of leaf extracts, three 5-6 week old plants per replicate were ground in 3 volumes of Extraction Buffer (EB) (50 mM MOPS pH 7.0 and 5 mM EDTA) with sand. After centrifugation at 4°C for 10 min (10,000 RPM), the soluble fraction was assayed for total β-amylase activity in 0.5 mL 50 mM MES (pH 6.0) and 10 mg/mL soluble starch for 30 min at 22°C. For assays of recombinant proteins, purified proteins were suspended in EB gelatin (50 mM MOPS pH 7.0 and 1 mg/mL gelatin) and treated with 5 mM DTT for 20 min. The enzyme suspensions with DTT were then diluted 500-fold before treatment with 0.5 mM GSNO or water (control) for 15 min. The GSNO- or water-treated enzymes were assayed for 20 min at 20°C. Assays of leaf extracts and recombinant proteins were stopped by immersion into a boiling water bath for 3 min. The production of reducing sugars was measured by the Somogyi-Nelson assay

(Nelson 1944) using maltose as the standard. The concentrations of proteins were measured using the Bio-Rad Protein Assay Kit with bovine serum albumin as the standard.

QuikChange Mutagenesis

Site-directed mutagenesis via the QuikChange method (Agilent Technologies) was used to make the BAM1 and BAM3 mutants. Mutagenesis primers had the nucleotide substitution with about 20 nucleotides on either side that matched the BAM1 or BAM3 template (Table 1). The over-expression vector pET29a containing the BAM1 or BAM3 coding sequence attached to His tags (described in Monroe et al. 2014) was used as the template for the BAM1 and BAM3 mutants, respectively. Once the plasmids were amplified with the mutagenesis primers via PCR, the PCR products were digested with Dpn1 for 1.5 hours at 37°C to degrade any unamplified template and transformed into DH5α *E. coli* cells. The plasmids were then isolated and sequenced by Eurofins Genomics to confirm if the nucleotide substitutions were successful. Confirmed plasmids were transformed into BL21+ *E. coli* cells for over-expression and purification.

Protein Purification

The pET29a plasmids containing the BAM1 and BAM3 WT sequences or mutations were over-expressed in BL21+ *E. coli* cells. The cells were grown in LB media supplemented with 50 µg/mL kanamycin at 37°C with shaking at 250 rpm. Once the cells reached an optical density of 0.45 at 600 nm, 1.0 mM IPTG was added to induce expression of the protein, and the cells were transferred to a 20°C incubator. After shaking overnight, the cells were centrifuged at 4°C and 8000 rpm for 15 min. Sonication was then used to lyse the cells, which were suspended in 35mL of binding buffer (50 mM pH 8.0 NaH_2PO_4, 0.3 M NaCl, and 10 mM imidazole). The supernatant from centrifugation (9000 RPM for 15 min at 4°C) was incubated with nickel-

nitrilotriacetic acid agarose His-Bind Resin (QIAGEN) for 1.5 hours at 4°C. Once the beads were rinsed by centrifugation and suspended in 10mL binding buffer, they were loaded into a purification column. To remove the unbound proteins, 20x the bead volume of wash buffer (50 mM pH 8.0 NaH_2PO_4, 0.3 M NaCl, and 40 mM imidazole) was added. Then, 10x the bead volume of elution buffer (50 mM pH 8.0 NaH_2PO_4, 0.3 M NaCl, and 200 mM imidazole) was added. The elution fraction was then dialyzed overnight in 2 L of20 mM MOPS pH 7.0, 0.1 M NaCl, and 0.2 mM TCEP. Once the imidazole salts were removed, the protein solutions were concentrated with an Amicon Ultra-4 10K filter and stored at -80°C. Protein purity was assessed using Coomassie-Blue-stained SDS-PAGE gels.

Table 1: Mutagenesis primers. Forward and reverse primers for each mutant with the codons in red encoding the new amino acid.

Mutant	Primers
B3 H430D	Forward: AAGACGGGGAGCAACCTGAGGACGCGAATTGCTCACCAGAAGG Reverse: CCTTCTGGTGAGCAATTCGCGTCCTCAGGTTGCTCCCCGTCTT
B3 N432L	Forward: GGGAGCAACCTGAGCACGCGCTTTGCTCACCAGAAGGTCTGGT Reverse: ACCAGACCTTCTGGTGAGCAAAGCGCGTGCTCAGGTTGCTCCC
B3 S434A	Forward: AACCTGAGCACGCGAATTGCGCACCAGAAGGTCTGGTCAAGCA Reverse: TGCTTGACCAGACCTTCTGGTGCGCAATTCGCGTGCTCAGGTT
B1 D430H	Forward: GGGATCACGAACAGCCTCAACACGCACTTTGTGCACCAGAGAA Reverse: TTCTCTGGTGCACAAAGTGCGTGTTGAGGCTGTTCGTGATCCC
B1 L432N	Forward: ACGAACAGCCTCAAGACGCAAATTGTGCACCAGAGAAGCTAGT Reverse: ACTAGCTTCTCTGGTGCACAATTTGCGTCTTGAGGCTGTTCGT
B1 A434S	Forward: AGCCTCAAGACGCACTTTGTTCACCAGAGAAGCTAGTTAACCA Reverse: TGGTTAACTAGCTTCTCTGGTGAACAAAGTGCGTCTTGAGGCT

Sequence Alignments and Homology Models

The BAM1 and BAM3 sequences from a variety flowering plants were obtained by BLAST (Table 2). Sequences that were most similar to the BAM1 and BAM3 Arabidopsis sequences were aligned using Clustal Omega (Sievers et al. 2011). The sequence alignment was then visualized with BoxShade v3.2.

I-TASSER used the amino acid sequence of BAM1 and BAM3 without their predicted plastid transit peptide coding regions (BAM1, 41 amino acids and BAM3, 55 amino acids as described by Fulton et al. [2008]) to generate homology models (Yang et al. 2015; Roy et al. 2010; Zhang 2008). The homology models were then visualized with YASARA (Krieger and Vriend 2014).

Table 2: BAM3 and BAM1 orthologous sequence names

Organism	BAM3	BAM1
Arabidopsis thaliana	NP_567523.1	NP_189034.1
Solanum pennellii	XP_004244551.1	XP_015088061.1
Fragaria vesca	XP_004300297.1	XP_004296549.1
Citrus sinensis	XP_006477060.1	XP_006493994.1
Glycine max	NP_001236350.1	XP_003534086
Cucumis melo	XP_008448789.1	XP_008438436.1
Vitis vinifera	XP_002282871.1	XP_002285569.1
Populus trichocarpa	XP_006385389.1	XP_002314522.1
Ricinus communis	XP_002517513.2	XP_002518196.1
Phaseolus vulgaris	XP_007155732.1	XP_007152599.1
Beta vulgaris	XP_010695452.1	XP_010666969
Brachypodium distachyon	XP_003574353.1	XP_003558837.1
Sorghum bicolor	XP_002464915.1	XP_002468533.1
Setaria italica	XP_004983616.1	XP_004985750.1
Amborella trichopoda	XP_011621487	XP_006851336.1

Results

NO-induced modification of BAM3 may lead to its inhibition during cold stress in vivo

Of the nine BAMs in Arabidopsis, BAM1, 2, 3, 5, and 6, are catalytically active with BAM5 being cytosolic and the other active BAMs being plastidic (Monroe and Priess 1990; Fulton et al. 2009; Li et al. 2009; Monroe et al. 2014). Monroe et al. (2014) sought to characterize the properties of the active BAMs *in vivo*. The relative contributions of the plastidic BAMs were previously difficult to measure due to the high activity of the cytosolic BAM5 masking the other isozymes, but Monroe et al. (2014) made a series of double mutant plants lacking BAM5 and one of the other active BAMs using T-DNA insertion lines from the ABRC. Based on these mutants, it was found that BAM3 was the predominant plastidic BAM in leaf extracts of pre-flowering plants with BAM1 playing a minor role, probably because there are many fewer guard cells, which is where BAM1 is found, than mesophyll cells, which is where BAM3 is found. Therefore, BAM3 and BAM1 contribute most of the β-amylase activity in pre-flowering *bam51* and *bam53* plants, respectively, with BAM2 and BAM6 having a larger role in older plants (Monroe et al. 2014). The cold-stress induced transcription of *BAM3* observed by Kaplan and Guy (2004) was supported by Monroe et al. (2014), but they also found a decline in β-amylase activity in *bam5* and *bam53* plants, suggesting that BAM3 activity decreases under cold stress.

While experiments with the plant double mutants led to convincing results, the effects of BAM2 and BAM6 cannot be ignored. By crossing a series of homozygous single BAM knockouts, allowing self-pollination, and confirming homozygotes with PCR, two triple mutants, *bam516* and *bam536,* were made so that only β–amylase activity contributed by BAM3 and BAM1, respectively, could be measured. Activity from BAM2 could be ignored because our

assays do not include salt, which our lab recently found is a prerequisite for BAM2 activity. Some of the experiments performed in Monroe et al. (2014) dealing with the response of the *bam51* and *bam53* double mutants to cold stress were repeated with the *bam516* and *bam536* triple mutants. It was again found that BAM3 activity in *bam516* plants was inhibited under cold stress but BAM1 activity in *bam536* plants was unaffected (data not shown). Post-translational inhibition of BAM3 could explain the high levels of *BAM3* transcript yet low levels of BAM3 protein activity.

Due to the known role of NO signaling in cold-stressed plants, it was hypothesized that NO-induced modification of BAM3 could result in the inhibition of BAM3 under cold stress. To determine if NO decreases the activity of BAM3 in the absence of cold stress, I treated Arabidopsis plants with sodium nitroprusside (SNP), a compound that releases NO in the form of nitrosonium cations when treated with light irradiation (Lum et al. 2005). After treating the triple mutants with 2 mM SNP for 5 hours and assaying β-amylase activity in the crude leaf extract, I showed that SNP significantly decreased the BAM3 activity in *bam516* by about 80% but had no significant effect on BAM1 activity in *bam536* (Figure 1). Modification of proteins by GSNO is a NO-induced mechanism of action and the results from the SNP experiment are consistent with the inhibition of purified BAM3 by GSNO by 80% *in vitro*, suggesting that the mechanism of cold stress-induced inhibition of BAM3 *in vivo* may be modification by GSNO.

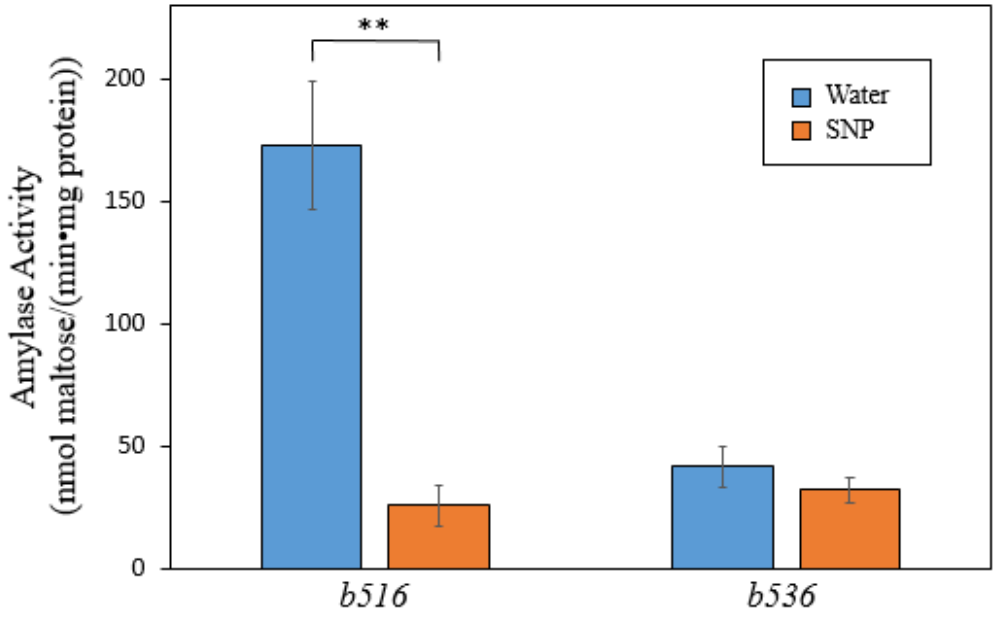

Figure 1: Effect of SNP on BAM1 and BAM3 activity. Triple mutants *bam516* and *bam536* were used to measure BAM3 and BAM1 activity, respectively. Plants were sprayed with 2 mM SNP or water (control) and harvested after 5 hours of exposure. Crude extracts were assayed at 22°C with soluble starch as the substrate. Values are means ± SD (n=3). ** indicates statistical significance ($p<0.01$).

Comparison of the microenvironment around C^{433} in BAM1 and BAM3

Studies of single BAM3 mutants in which cysteine residues were replaced with either Ser or to the corresponding BAM1 residue revealed that C^{433} in BAM3 is modified by GSNO (Storm et al., unpublished). Because the corresponding BAM1 amino acid at position 433 is also a cysteine, I compared sequence alignments of BAM1 and BAM3 in different species and generated homology models in order to determine any differences in the microenvironment surrounding C^{433} in BAM1 and BAM3.

A comparison of the 10 amino acids on either side of C^{433} in BAM1 and BAM3 revealed conserved similarities and differences among the BAM1 and BAM3 orthologs from a variety of flowering plant species, including eleven eudicots, three monocots, and the primitive flowering plant *Amborella trichopoda* (Figure 2). Conserved differences may help to explain the sensitivity

of C^{433} in BAM3 to GSNO and insensitivity of C^{433} in BAM1, assuming the BAM1 orthologs and BAM3 orthologs have similar properties as their respective BAM1 and BAM3 counterparts in Arabidopsis. Most notably, positions 430, 432, and 434 in BAM1 have a highly conserved Asp, Leu, and Ala residue, respectively, whereas the corresponding amino acids in BAM3 are His, Asn, and Ser, respectively. Interestingly, while D^{430} in BAM1 is perfectly conserved among the species selected, H^{430} in BAM3 is less well conserved. However, BAM3 has more conserved residues at positions 432 and 434 than BAM1. Other conserved differences around C^{433} include the highly conserved H^{425} and K^{437} in BAM1 and the corresponding residues in BAM3, G^{425} and G^{437}. The effects of positions 425 and 437 in making BAM3 sensitive to GSNO and BAM1 insensitive to GSNO were already tested by our lab, and it was found that they contribute little if at all to the sensitivity and insensitivity of BAM3 and BAM1, respectively, to GSNO (data not shown). Therefore, based on sequence alignments alone and the assumption that conserved differences could help lead to a difference in the microenvironment around C^{433} in BAM1 and BAM3, it seems that residues at positions 430, 432, and 434 may be potentially important.

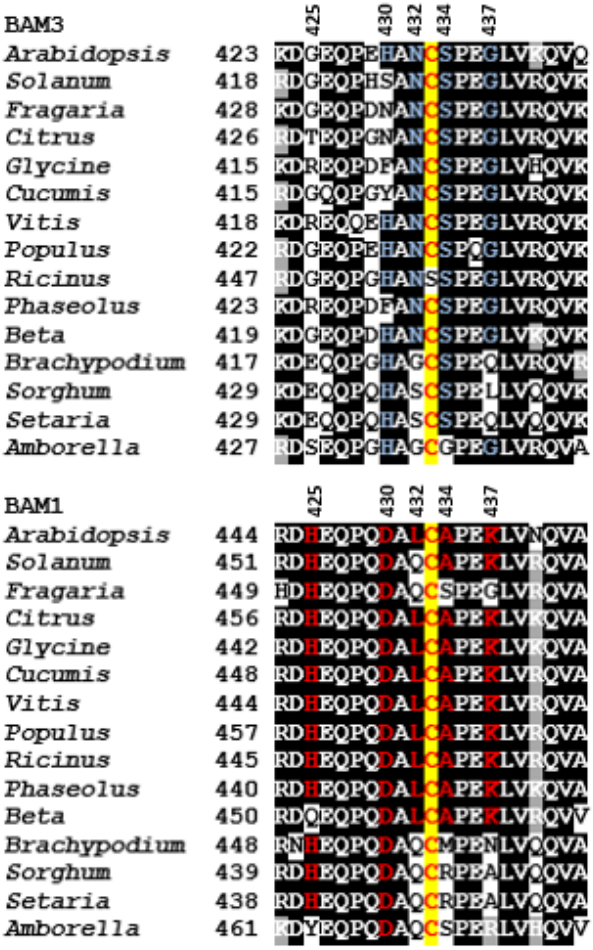

Figure 2: Sequence alignments of BAM3 and BAM1 around C^{433} (highlighted yellow). Black, gray, and white backgrounds represent highly conserved, semi-conserved, and non-conserved residues, respectively. The blue- and red-colored amino acids in the BAM3 and BAM1 set, respectively, represent conserved differences between BAM3 and BAM1. The numbers 425, 430, 432, 434, and 437 indicate the Arabidopsis BAM3 numbering of the potentially important residues. The eudicots selected are *Arabidopsis thaliana*, *Solanum pennelli*, *Fragaria vesca*, *Citrus sinensis*, *Glycine max*, *Cucumis melo*, *Vitis vinifera*, *Populus trichocarpa*, *Ricinus communis*, *Phaseolus vulgaris*, and *Beta vulgaris*. The monocots are *Brachypodium distachyon*, *Sorghum bicolor*, and *Setaria italica*; *Amborella trichopoda* is a primitive flowering plant. Sequences were obtained using BLAST and the BAM3 (At4G17090) and BAM1 (At4G15210) genes from Arabidopsis. Clustal Omega was used to align the sequences.

While sequence alignments of the primary structure can offer important information about conserved amino acids, the secondary and tertiary structures ultimately affect the microenvironment. To view the 3D structure around C^{433}, I generated homology models of BAM1 and BAM3 using I-TASSER (Yang et al. 2015; Roy et al. 2010; Zhang 2008). Both of the BAM1 and BAM3 models from I-TASSER were based on the crystal structure of BAM5 purified from soybean (PDB-ID 1V3H). I visualized structures of BAM1 and BAM3 from I-TASSER using YASARA (Krieger and Vriend 2014) (Figures 3 and 4). The similarity between BAM1 and BAM3, shown by an RMSD of 0.325 Å over 447 aligned residues between the homology models, suggests that glutathionylation of C^{433} in BAM1 could interfere with starch binding as it does in BAM3 (Figure 3). Because treatment of BAM1 with GSNO had no effect on activity, it is likely that C^{433} is not glutathionylated in BAM1 as opposed to being glutathionylated but not affecting activity. In the homology models, the catalytic residues Glu259 and Glu456 (numbering based on BAM3) are highlighted to show the location of the active site (Kang et al. 2004). Figure 4A, C, and E highlights the orientations of H^{430}, N^{432}, and S^{434} in BAM3, respectively, while figure 4B, D, and F shows D^{430}, L^{432}, and A^{434} in BAM1, respectively. The conserved amino acids at positions 432 and 434 in both BAM1 and BAM3 are oriented away from C^{433} in the homology models. Both of those amino acids in BAM3 have polar uncharged side chains while the corresponding residues in BAM1 are hydrophobic. Interestingly, at position 430, His in BAM3 is pointed away from C^{433} whereas Asp in BAM1 is facing the thiol group of C^{433}. Histidine can be positively charged, which could help attract GSNO and/or function as a hydrogen bond donor through a network of water molecules. Aspartate is negatively charged, which could help repel GSNO and/or disfavor the negatively-charged thiolate form of C^{433} in

BAM1. Therefore, based on the homology models, the residue at position 430 may be more important than the residues at 432 and 434 to affect the microenvironment around C^{433}.

The primary structure around C^{433} can help determine important residues, but amino acids that are distant from C^{433} in the primary structure may be close to it in the tertiary structure. There is a loop that is near the one with C^{433}, which contains histidines at positions 376 and 378 in both BAM1 and BAM3. Because these residues are conserved in both isozymes, it is not likely that these positions could explain the different sensitivities of C^{433} in BAM1 and BAM3 to GSNO. Residues that are close to C^{433} in the tertiary structure are just as likely to influence C^{433}, but no differences were found in the tertiary structure near C^{433} that could not be found within 10 amino acids in the primary structure.

Web-based prediction of glutathionylation sites

The website GSHsite (http://csb.cse.yzu.edu.tw/GSHSite/index.php) predicts the likelihood of glutathionylation of cysteines by using the 10 amino acids before and after Cys residues. The predictions from GSHsite are based on the primary structure surrounding experimentally-identified glutathionylation sites from mouse macrophages. GSHsite produces a metric that represents the relative sensitivity of cysteines to GSNO and thus has no units. For example, GSHsite predicted C^{433} in BAM1 and BAM3 to have a sensitivity metric of 1.00 and 1.87, respectively (Table 2). While this is consistent with the sensitivity of BAM3 to GSNO and the insensitivity of BAM1, the website does not take into account the 3-D structure and microenvironment surrounding the Cys residue, which often alters the pKa of the thiol as well as the orientation of the approaching GSNO molecule.

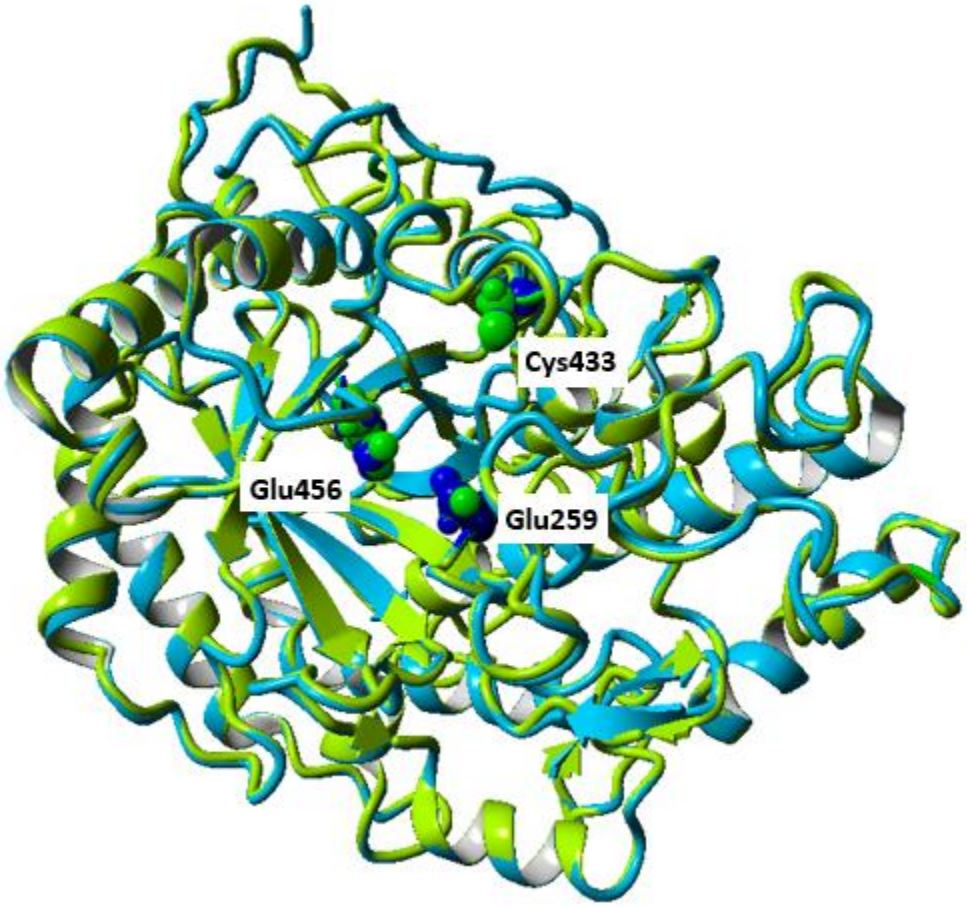

Figure 3: Alignment of the BAM3 and BAM1 homology models. BAM3 is colored blue and BAM1 is colored green. Lighter colors represent the protein backbone and darker colors highlight Cys433 and the two catalytic Glu residues at positions 259 and 456 to indicate the location of Cys433 relative to the active site. The models were aligned using YASARA.

A.

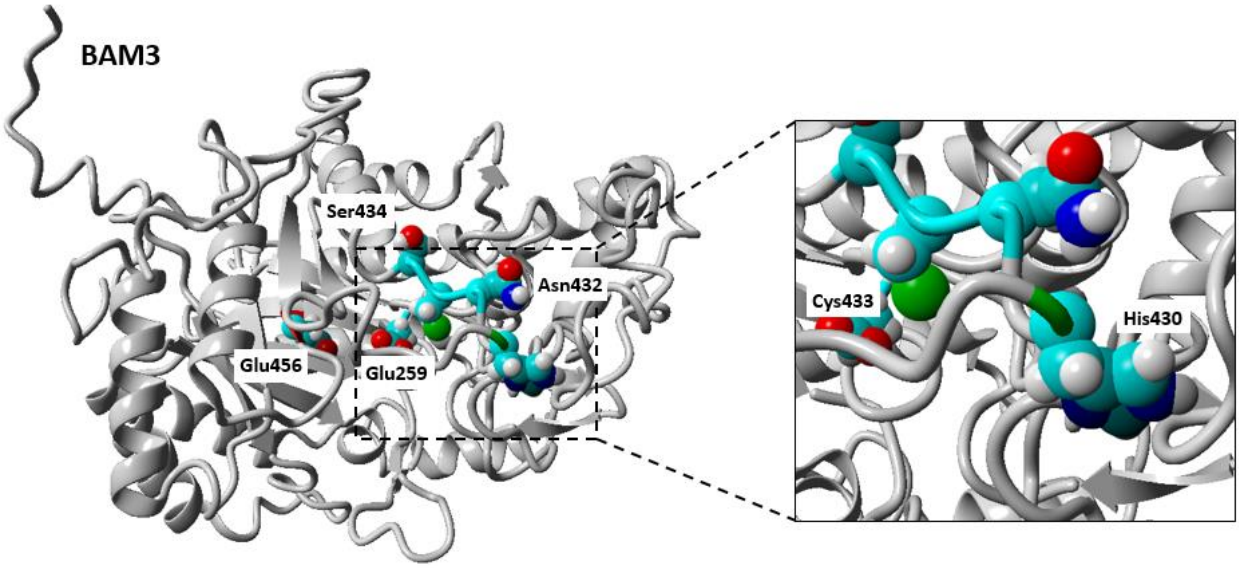
BAM3
Ser434
Asn432
Glu456
Glu259
Cys433
His430

B.

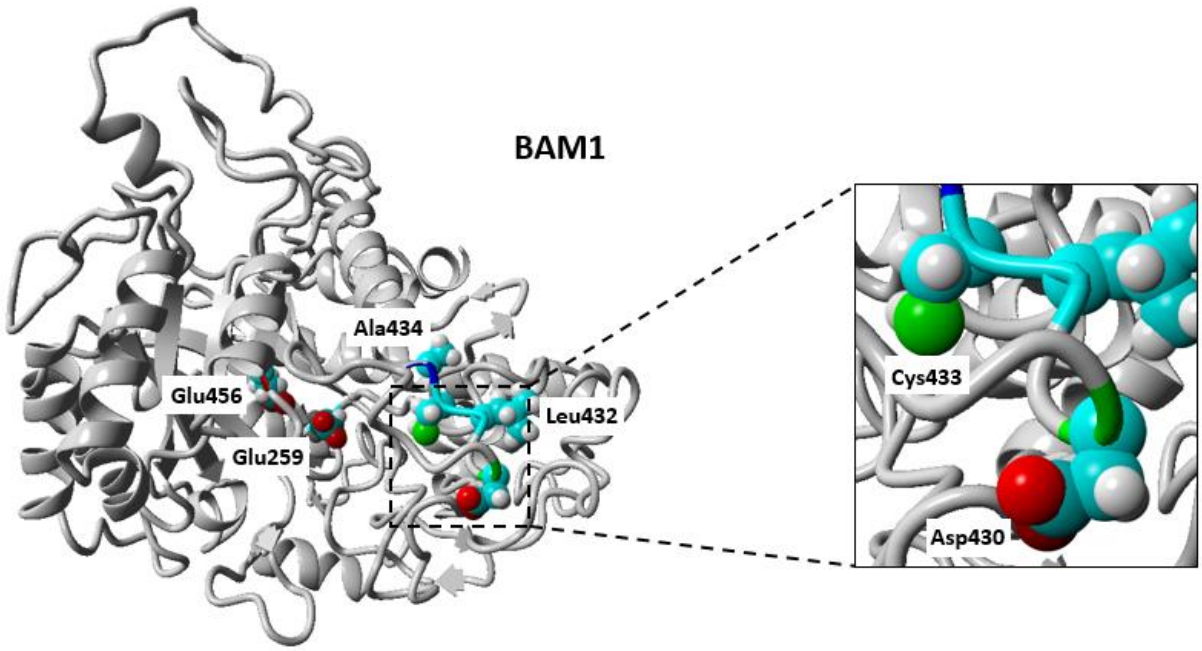
BAM1
Ala434
Glu456
Leu432
Glu259
Cys433
Asp430

C.

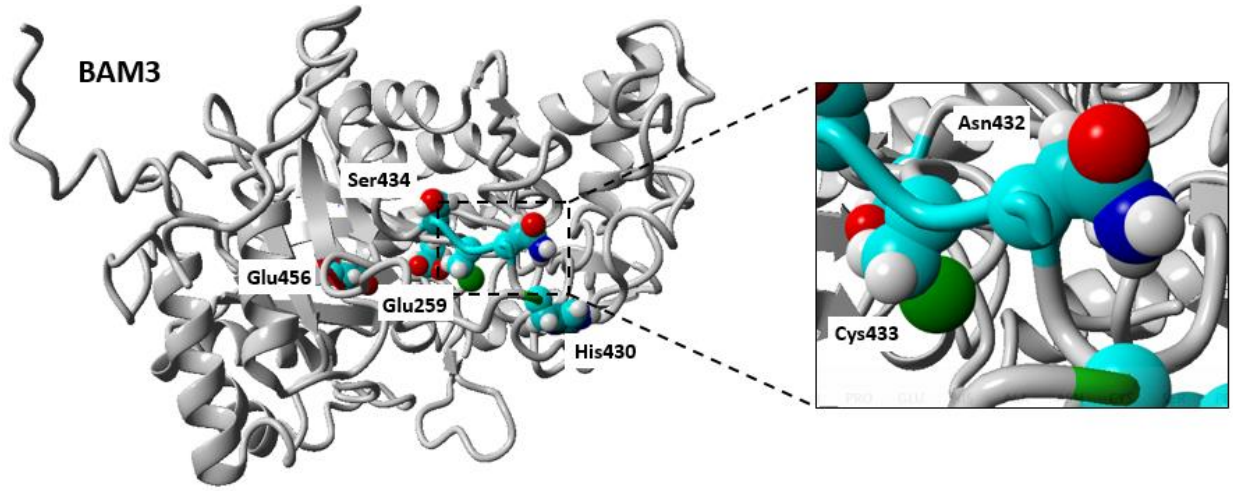
BAM3
Ser434
Glu456
Glu259
His430
Asn432
Cys433

D.

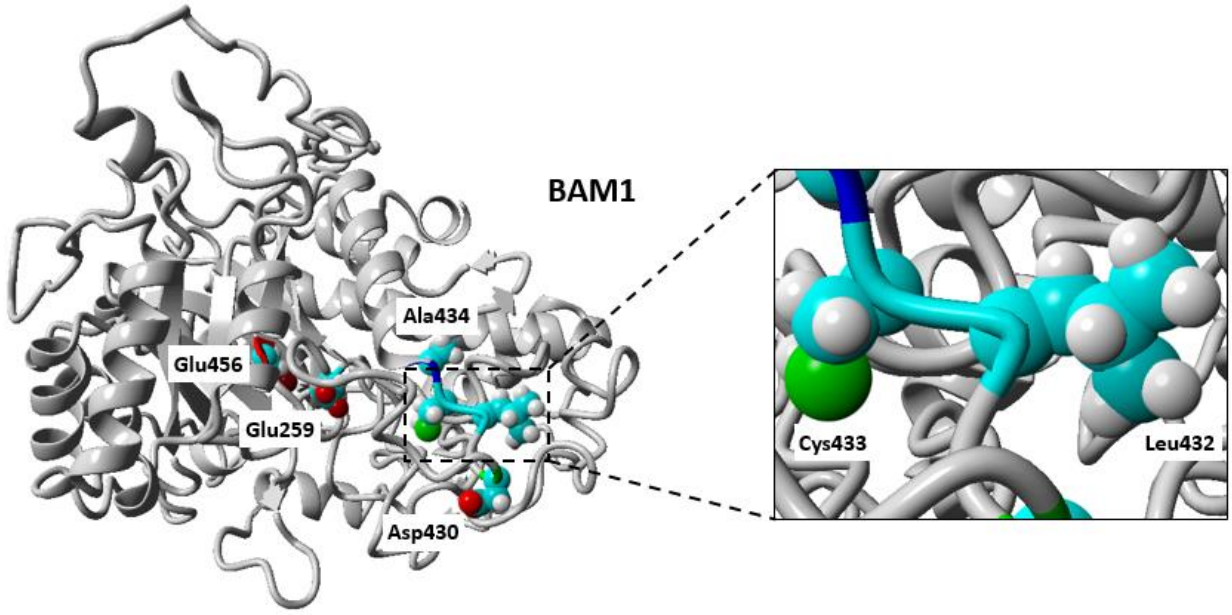
BAM1
Ala434
Glu456
Glu259
Asp430
Cys433
Leu432

E.

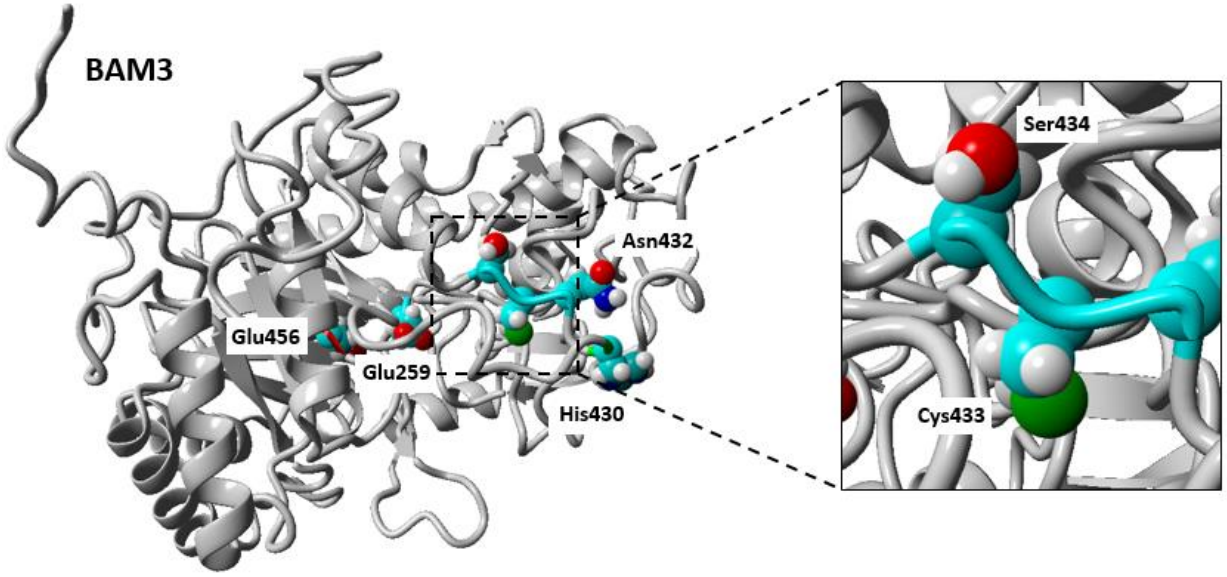

F.

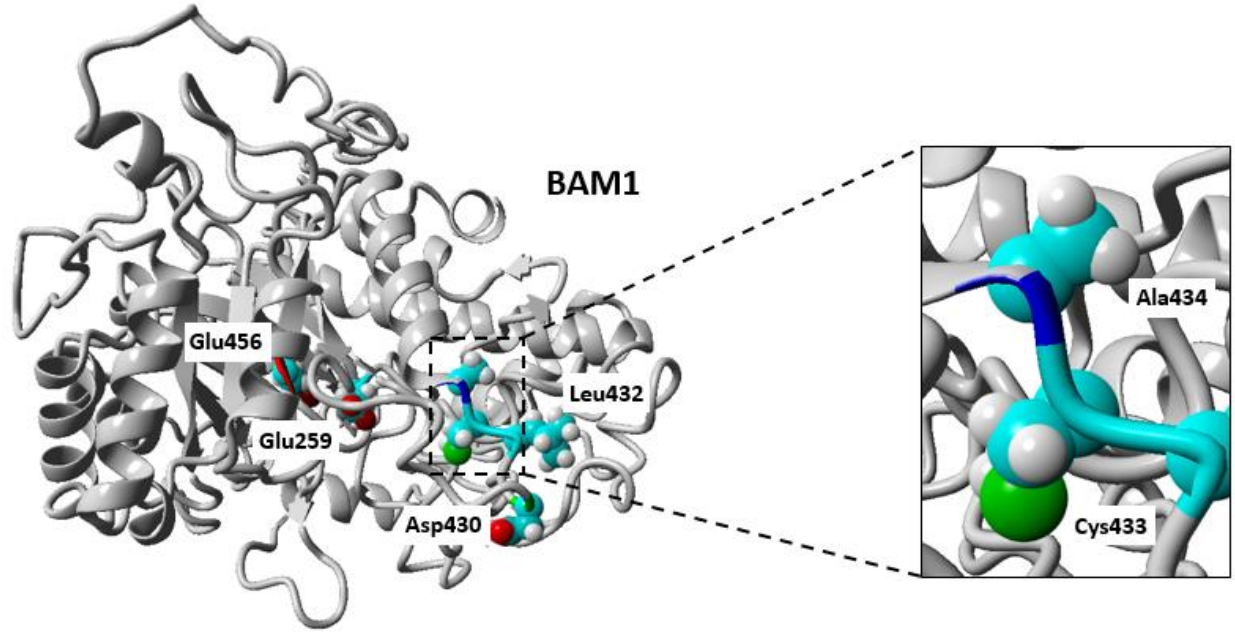

Figure 4: Homology models of BAM3 and BAM1. **A**, orientation of H^{430} relative to C^{433} in BAM3. **B**, orientation of D^{430} relative to C^{433} in BAM1. **C**, orientation of N^{432} relative to C^{433} in BAM3. **D**, orientation of L^{432} relative to C^{433} in BAM1. **E**, orientation of S^{434} relative to C^{433} in BAM3. **F**, orientation of A^{434} relative to C^{433} in BAM1. The catalytic residues, Glu259 and Glu456, are highlighted to show the location of the active site. Light blue, white, green, blue, and red balls correspond to carbon, hydrogen, sulfur, nitrogen, and oxygen, respectively. Models were generated by I-TASSER and visualized with YASARA. Numbers are based on BAM3.

Nevertheless, I was interested in how the GSHsite prediction for C^{433} was affected by the potentially important amino acids in making BAM3 sensitive and BAM1 insensitive to GSNO based on the sequence alignment. The 10 amino acids on either side of C^{433} in BAM3 and BAM1 were entered into GSHsite (Table 3). To test the effect of positions 430, 432, and 434 on the GSHsite predictions of C^{433} glutathionylation, BAM3 sequences with amino acid substitutions from one of the conserved residues to the corresponding residue in BAM1 were entered into GSHsite. Similarly, BAM1 sequences with amino acid substitutions from one of the conserved residues to the corresponding residue in BAM3 were also entered into GSHsite. Among the BAM3 single mutants, GSHsite predicted that C^{433} would be less sensitive to glutathionylation after any of the three substitutions, but that C^{433} would be the least sensitive to glutathionylation by converting N^{432} to Leu in BAM3 (BAM3-N432L). GSHsite also predicted that converting D^{430} to His (BAM1-D430H) and L^{432} to Asn (BAM1-L432N) would make C^{433} in BAM1 more sensitive to glutathionylation by GSNO than the WT. Interestingly, C^{433} the BAM1-A434S mutant was predicted to be more insensitive to GSNO than with the WT BAM1 sequence.

Table 3: The predicted likelihood of glutathionylation of C^{433} in BAM3 and BAM1 mutants compared to the WT forms. Predictions obtained from GSHsite (http://csb.cse.yzu.edu.tw/GSHSite/index.php) using the 10 amino acids before and after C^{433}.

Protein	Score
BAM3 WT	1.87
BAM3-H430D	1.41
BAM3-N432L	1.34
BAM3-S434A	1.70
BAM1 WT	1.00
BAM1-D430H	1.25
BAM1-L432N	1.20
BAM1-A434S	0.88

Purification and specific activity of BAM1 and BAM3 mutants

Based on the sequence alignments around C^{433} in BAM1 and BAM3 and the homology models of those enzymes, the amino acids at positions 430, 432, and 434 could potentially help make BAM3 sensitive to GSNO and BAM1 insensitive to GSNO. GSHsite also predicted that these positions affect the sensitivity of BAM3 and insensitivity of BAM1 to glutathionylation by GSNO, except for position 434 in BAM1 (Table 3). If these amino acids are important in affecting the microenvironment, then replacing H^{430}, N^{432}, or S^{434} in BAM3 with the corresponding amino acids in BAM1, D^{430}, L^{432}, or A^{434}, respectively, should make the BAM3 mutants less sensitive to GSNO. Furthermore, replacing D^{430}, L^{432}, or A^{434} in BAM1 with the

corresponding amino acids in BAM3 should make the BAM1 mutants more sensitive to GSNO. Therefore, I sought to make six mutants: BAM3-H430D, BAM3-N432L, BAM3-S434A, BAM1-D430H, BAM1-L432N, and BAM1-A434S, and test their sensitivity to GSNO.

I performed site-directed mutagenesis on BAM1 and BAM3 using the QuikChange method. I made forward and reverse primers for each mutation that matched either the BAM1 or BAM3 template embedded within an overexpressing vector so that the protein contained a His-tag (Table 1). I used the WT BAM1 template for the BAM1 mutants, but I used a previously made C177V/C257A template for the BAM3 mutants. Because it was found that C^{177} and C^{257} increase the GSNO sensitivity of C^{433} in BAM3 without being glutathionylated themselves, making BAM3 mutants in a template that had Val and Ala instead of C^{177} and C^{257}, respectively, removed any effects from C^{177} and C^{257} on the sensitivity of C^{433} in BAM3. Therefore, the three BAM1 mutants are just single mutants, but the three BAM3 mutants are actually triple mutants (for clarity, the BAM3 triple mutants are indicated by the mutation around C^{433} and a $^{+}$ to refer to the C177V/C257A substitutions; i.e. BAM3-C177V/C257A/H430D is $BAM3^{+}$-H430D). Once the template was confirmed to be amplified via PCR by gel electrophoresis, the PCR product was then transformed into competent *E.coli* cells. The overexpression vector was isolated using a mini prep and was then sequenced to confirm that the mutation was inserted correctly. Finally, the plasmid was transformed into BL21+ *E. coli* cells for protein expression. Proteins were then purified using affinity chromatography using the fused His-tag. An SDS-PAGE gel was performed with samples from different steps of the purification process to show the enrichment of the $BAM3^{+}$-H430D mutant (Figure 5A). The pre-IPTG-induced sample had faint bands, but the post-induced sample had more distinct bands with an especially strong band at the same position as the band in the lane with the elution sample. The elution sample was overloaded and

there was only one band at about 55 kDa, the expected size for BAM3, indicating that the sample was pure. Another gel was performed to show the successful purification of all six BAM3 and BAM1 mutants (Figure 5B). The BAM3 mutants were loaded into the first three lanes, each of which had a single band at about 55 kDa. However, the BAM1 mutants had two bands close to each other centered on 65 kDa, the expected size of BAM1. When BAM1 WT and other mutants are purified by our lab, we usually see this double band. It is likely that the BAM1 proteins were not denatured fully, and there are two structural states, possibly due to the redox sensitivity of BAM1, that result in two bands. Fulton et al. (2008) found that the WT forms of BAM1 and BAM3 migrated as 67.5 kDa and 55.5 kDa, respectively, consistent with how my BAM1 and BAM3 mutants migrated.

After I made the six mutant proteins, I measured their specific activity (Figure 6). Each mutant was pre-treated with 5 mM DTT to fully reduce any disulfide bonds. The WT BAM1 was about two times as active as WT BAM3, which was also observed by Fulton et al (2008) and Li et al. (2009). The BAM1 mutants were about half as active as the wild-type and all had similar activity. The BAM3 mutants, however, were much more variable in their activity. The only BAM3 triple mutant that was highly active was $BAM3^{+}$-H430D with about 80% of the activity of the BAM3-C177V/C257A double mutant control. $BAM3^{+}$-N432L had no activity whereas $BAM3^{+}$-S434A was only slightly active. After purifying those latter two mutants multiple times, even batches with a higher concentration of protein yielded the same results. It is possible that these two BAM3 mutants have little to no activity because the combination of substitutions at positions 177, 257, and 432 or 434 makes the mutant enzymes inactive. Most recently, a new set of BAM3 mutants were made in a completely wild-type BAM3 background, which contains C^{177} and C^{257}. Those BAM3 single mutants, BAM3-H430D, BAM3-N432L, and BAM3-S434A, all

had activity in test assays (data not shown), suggesting that the mutations at 177, 257, and 432 or 434 changed the structure of the BAM3^{+}-N432L and BAM3^{+}-S434A mutants, respectively, enough to affect activity or that there were issues in the purification process.

A.

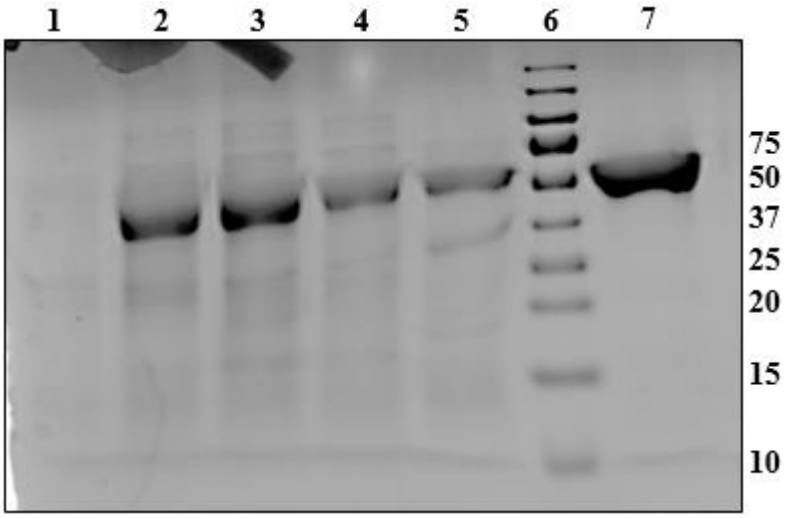

B.

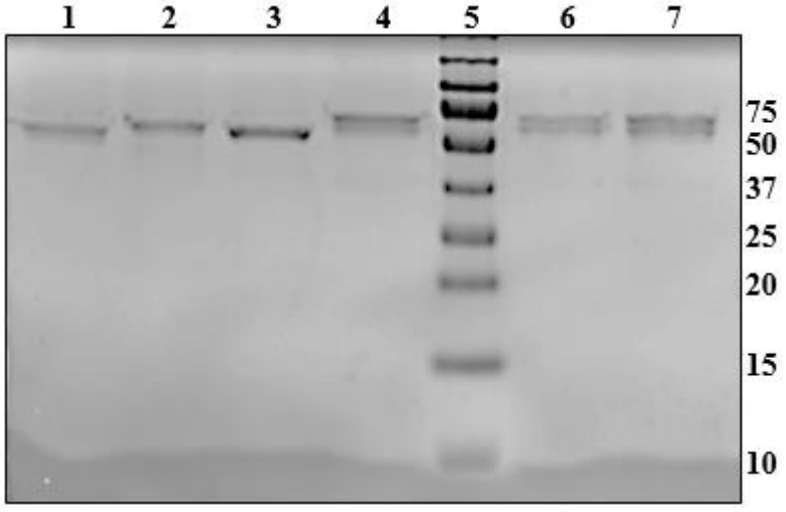

Figure 5: SDS Polyacrylamide gels of BAM3 and BAM1. **A**, Representative purification process for BAM3^{+}-H430D; pre-induced sample (lane 1), post-induced sample (lane 2), soluble lysate (lane 3), unbound fraction (lane 4), wash fraction (lane 5), marker (lane 6), and elution (lane 6). **B**, BAM3 and BAM1 mutants; BAM3^{+}-H430D (lane 1), BAM3^{+}-N432L (lane 2), BAM3^{+}-S434A (lane 3), BAM1-D430H (lane 4), marker (lane 5), BAM1-L432N (lane 6), BAM1-A434S (lane 6). Both protein gels used the same protein standard (in kDa) as a marker and were visualized with Coomassie Blue. Expected kDa for BAM1 and BAM3 are 67.5 and 55.5 kDa, respectively.

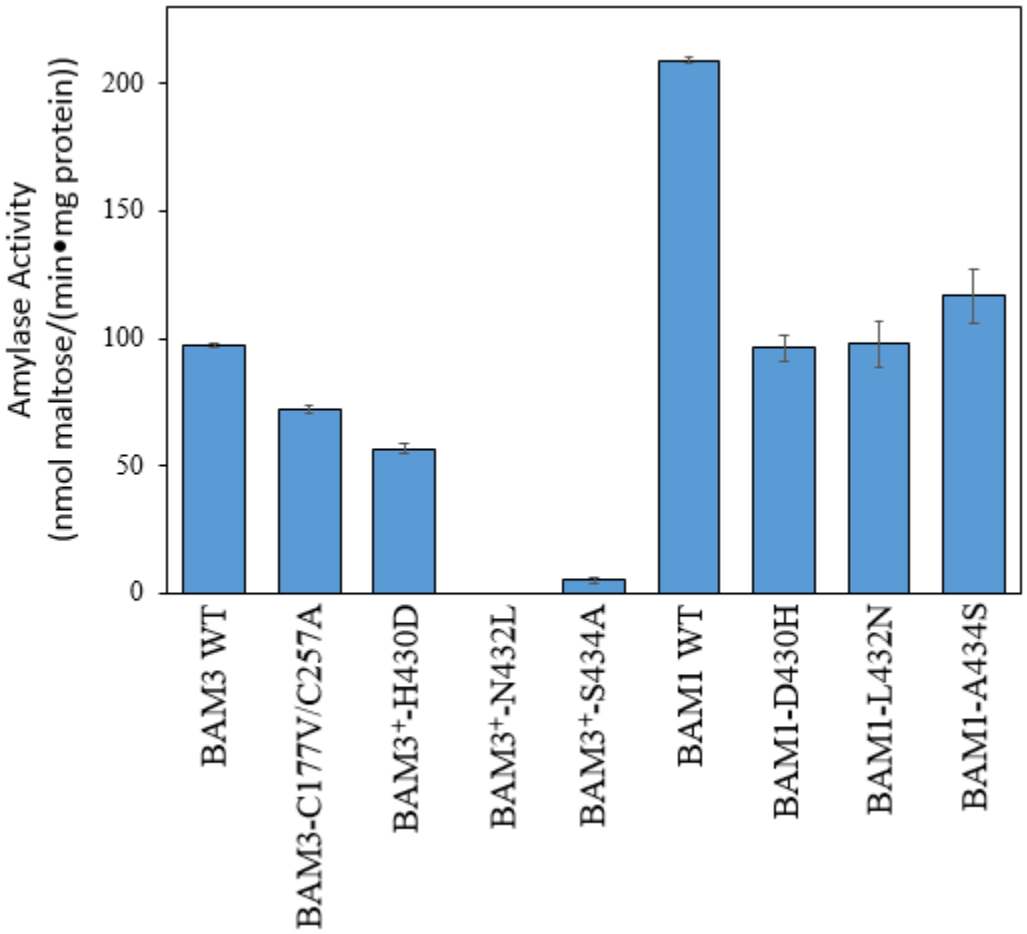

Figure 6: Specific activity of BAM3 and BAM1 mutants compared to the WT and double mutant controls. Each enzyme was pre-treated with 5mM DTT for 20 min and assayed at 22°C with soluble starch as the substrate. Amylase activity was standardized with the mg of protein used. Values are means ± SD (n=3).

Glutathionylation assays of BAM1 and BAM3 mutants

The active BAM1 and BAM3 mutants ($BAM3^{+}$-H430D, BAM1-D430H, BAM1-L432N, and BAM1-A434S) were then assayed with and without GSNO to determine whether the mutants differed in their sensitivity to GSNO compared to the WT or double mutant controls. Because DTT is necessary to fully reduce the enzymes but interferes with glutathionylation, the 5mM DTT pre-treatment had to be diluted before the enzymes were treated with GSNO. After testing the effect of DTT on BAM3 WT, it was determined that a 5 mM DTT pre-treatment fully activated BAM3 WT and that a 500-fold dilution of the DTT pre-treatment was required for maximal inhibition of GSNO (data not shown). Therefore, the enzymes pre-treated with 5 mM DTT were diluted 500-fold before 0.5 mM GSNO was applied.

To test the influence position 430 has on the glutathionylation of C^{433}, the $BAM3^{+}$-H430D mutant was compared to the BAM3-C177V/C257A control and the BAM1-D430H mutant was compared to the BAM1 WT control in their sensitivity to GSNO (Figure 7A). As expected, the BAM1 control was insensitive to GSNO, but the BAM3-C177V/C257A control was only inhibited by 25%. The BAM3 triple mutant was equally sensitive to the BAM3 control, but the BAM1 mutant was inhibited by GSNO by 45% ($p<0.05$). This indicates that Asp^{430} in BAM1 does play a role in making BAM1 insensitive to GSNO. It is hard to understand why the conversion of His^{430} to Asp in BAM3 did not make the BAM3 mutant less sensitive to GSNO, as the factors underlying the specificity of glutathionylation are not understood.

Because the BAM3 triple mutants that were made to test the influence positions 432 and 434 had on the sensitivity of BAM3 to GSNO were not active enough to do GSNO assays with, only the BAM1-L432N and BAM1-A434S mutants were tested (Figure 7B). The BAM1-L432N mutant was not statistically significantly inhibited by GSNO ($p=0.08$), but multiple experiments

have shown a consistent 15% inhibition. The BAM1-A434S mutant was inhibited by GSNO by over 20% (p=0.01). Whether positions 432 or 434 affect the sensitivity of BAM3 to GSNO cannot be determined using the triple mutants BAM3^{+}-N432L and BAM3^{+}-S434A as they were not active. An analysis of the effect of positions 430, 432, and 434 on the sensitivity of BAM3 to GSNO must wait until the BAM3 single mutants are tested, but it can be concluded that D^{430} in BAM1 had a greater effect on the insensitivity of BAM1 to GSNO compared to L^{432} and A^{434}, which may have minor roles.

A.

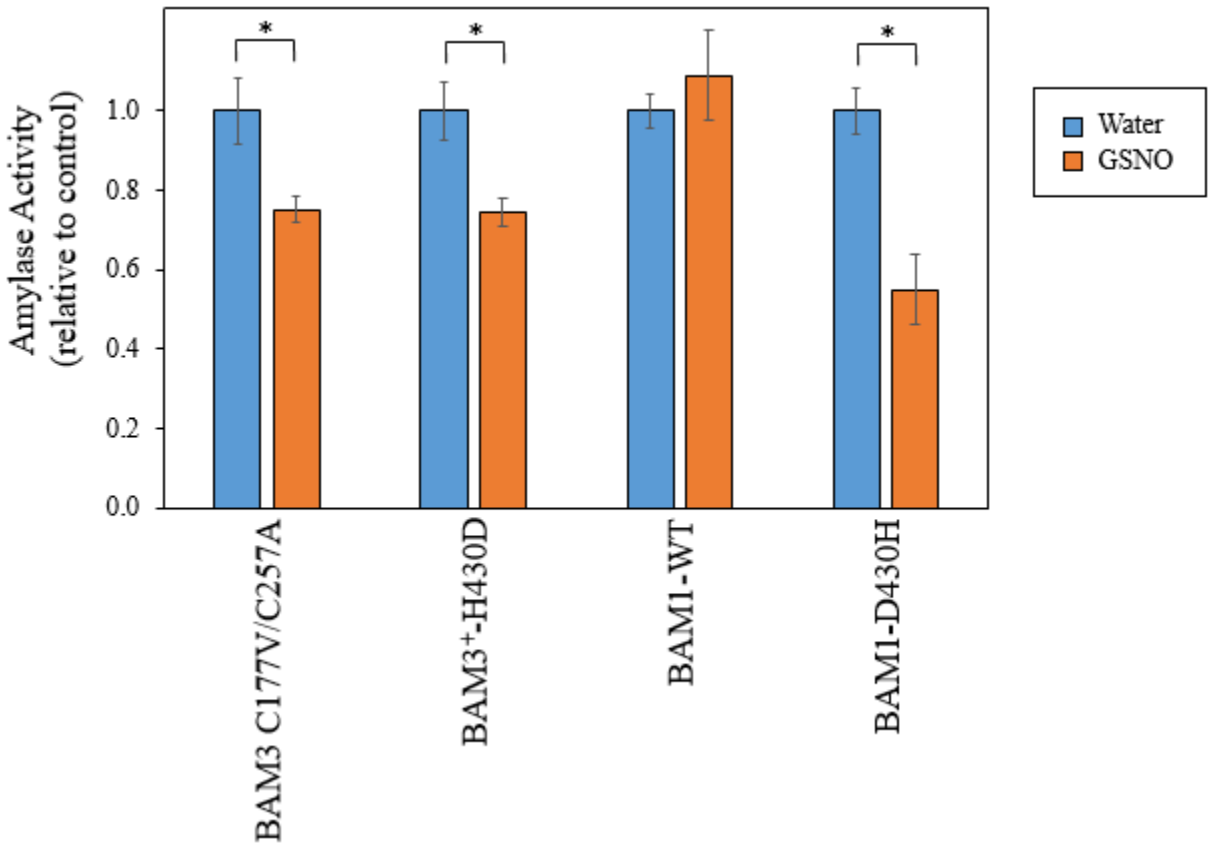

B.

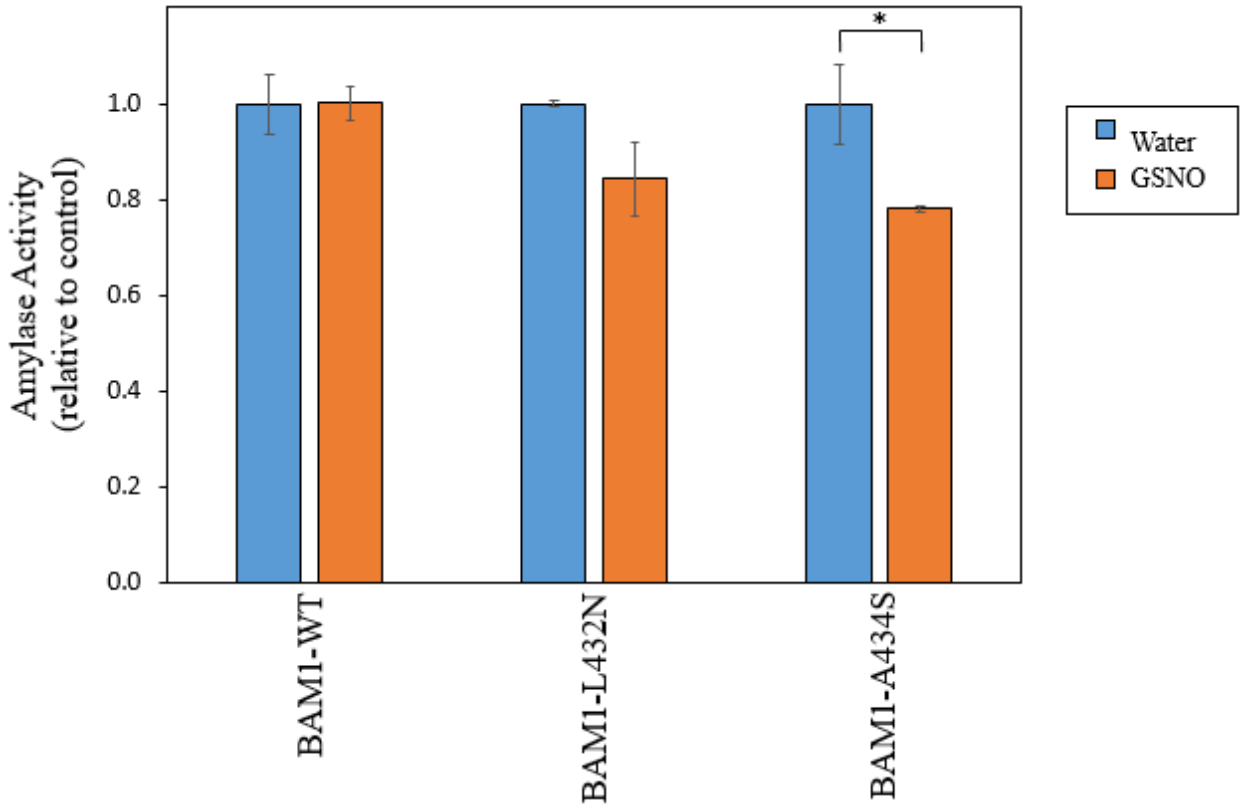

Figure 7: Amylase activity assays of GSNO-treated enzymes. **A**, Mutants of BAM3 and BAM1 at position 430 and the BAM3 C177V/C257A control and BAM1 WT control were treated with 0.5 mM GSNO or water and then amylase activity was measured. **B**, Mutants of BAM1 at positions 432 and 434 and the BAM1 WT control were treated with 0.5 mM GSNO or water and then amylase activity was measured. The activity of the GSNO-treated enzymes are relative to their respective water-treated enzymes, each standardized to one. Enzymes were pre-treated with 5 mM DTT, diluted 500-fold before the GSNO treatment, and assayed at 22° at 20 min. Values are means ± SD (n=3). * indicates statistical significance ($p<0.05$).

Discussion

The sensitivity of BAM3 to GSNO and insensitivity of BAM1 to GSNO at C^{433} raises a number of questions about the physiological and biochemical reasons for that difference. Physiologically, different cell-type specificities may, at least in part, explain why these two β-amylases are regulated differently. Biochemically, differences in the reactivity and accessibility of C^{433} based on surrounding amino acids in BAM1 and BAM3 could cause BAM1 to be insensitive and BAM3 to be sensitive to GSNO.

BAM1, at least in younger plants, is found primarily in guard cells, but BAM3 is localized to mesophyll cells. Cell-type specialization, a common feature of isozymes, may help to explain why BAM1 and BAM3 are not regulated in the same way under cold stress. While our lab's results do not yet confirm the inhibition of BAM3 via glutathionylation as the mechanism for decreased β-amylase activity under cold stress, results from multiple experiments may suggest that mechanism to be the case. First, it has been established that *BAM3* transcript increases during cold stress, but *BAM1* transcript remains unaffected (Kaplan and Guy 2004; Monroe et al. 2014). However, BAM3 activity decreases under cold stress whereas BAM1 activity is unaffected (Monroe et al. 2014; our unpublished results). Next, BAM3 activity *in vitro* is inhibited by GSNO, and the same treatment to BAM1 *in vitro* had no effect (our unpublished results). Finally, SNP treatment decreases BAM3 activity *in vivo* but had no effect on BAM1 activity (Figure 1). The inhibition of BAM3 by glutathionylation found *in vitro* could explain the results observed in cold- and SNP-treated plants, but further experiments are necessary to confirm glutathionylation as the mechanism. In fact, members in our lab are in the process of generating transgenic plants that are missing C^{433} in BAM3. If these transgenic plants do not accumulate starch and have little changes in BAM3 activity in response to cold stress, that would

provide evidence for the inhibition of BAM3 by modification of C^{433}, which is glutathionylated *in vitro*, under cold stress.

Assuming the mechanism of cold-stress induced inhibition of BAM3 is glutathionylation, the location of BAM1 in guard cells may explain why BAM1 is not inhibited by GSNO. NO plays a role in stomatal regulation and is present in guard cells not just during cold stress (Gayatri et al. 2013). GSNO, therefore, may be present as well, and it could continually inhibit BAM1 if it was sensitive to GSNO. Also, guard cells regulate stomatal opening and degrade starch during the day whereas mesophyll cells are the major photosynthesizing cells that degrade starch during the night, so it would not be expected for these cell types with different functions to respond to cold stress in the same way.

The sensitivity of cysteines to glutathionylation depends on the accessibility and reactivity of their thiol side chains. Because the homology models predict that C^{433} in both BAM1 and BAM3 are on a loop near the surface of the proteins, the difference in sensitivity of C^{433} to GSNO is not likely to be due to accessibility. In terms of reactivity, the N-terminal end of α-helices are known to stabilize the thiolate, or more reactive, form of cysteines through the donation of hydrogen bonds, increasing their susceptibility of glutathionylation (Miranda 2003). Interestingly, C^{433} in both isozymes are located near the N-terminal end of an α-helix, suggesting that the presence of an α-helix also cannot explain the differences in sensitivity. Therefore, other differences in the microenvironment around C^{433} in BAM3 and BAM1 revealed from the sequence alignment and homology models could explain the sensitivity and insensitivity of BAM3 and BAM1, respectively, to GSNO.

The amino acids that I predicted to be important in making BAM3 sensitive to GSNO based on the sequence alignment and side chain properties are H^{430}, N^{432}, and S^{434}. These amino

acids are all polar and could potentially stabilize the thiolate, or reactive, form of the C^{433} side chain by donating hydrogen bonds or forming favorable ionic interactions. Also, His can have a positively-charged side chain depending on its pKa, which could attract GSNO, a negatively-charged molecule. The corresponding amino acids in BAM1 are D^{430}, L^{432}, and A^{434}. Leu and Ala are both nonpolar, which could potentially raise the pKa of C^{433}, favoring the uncharged, less reactive thiol state. Asp has a negatively-charged carboxylate side chain at physiological pH, which could disfavor the negatively-charged thiolate form of C^{433} and/or help to repel an approaching GSNO molecule. Moreover, these amino acid residues are conserved among different species of flowering plants in their respective BAM1- and BAM3-like sequences.

To determine if these amino acids are important in making C^{433} sensitive to GSNO in BAM3 yet insensitive in BAM1, I made a series of BAM3 mutants that had amino acid substitutions to the corresponding residues in BAM1 and vice versa for a series of BAM1 mutants. In addition to the amino acid substitution at positions 430, 432, or 434, all of the BAM3 mutants had C177V and C257A substitutions to eliminate any effects C^{177} and C^{257} have on the sensitivity of C^{433} to glutathionylation. The only BAM3 triple mutant that was active enough for GSNO assays was $BAM3^{+}$-H430D whereas all of the BAM1 mutants were active (Figure 6). When $BAM3^{+}$-H430D and the corresponding BAM1 mutant, BAM1-D430H, were treated with GSNO, the BAM3 mutant was just as sensitive to GSNO as the BAM3-C177V/C257A control. However, BAM1-D430H was inhibited by 45% in the presence of GSNO while the BAM1 WT control was insensitive, suggesting that D^{430} plays a role in making BAM1 insensitive to GSNO and its conversion to the corresponding amino acid in BAM3 makes it sensitive (Figure 7A). We cannot say the same for H^{430} in BAM3 based on the mutants we used, in part because the BAM3-C177V/C257A control was not as sensitive as it was in previous tests. Of the other BAM1

mutants, only BAM1-A434S was significantly inhibited, but this inhibition was not as strong as that seen in the BAM1-D430H mutant (Figure 7B). This indicates that D^{430} has a greater effect on making C^{433} in BAM1 less sensitive to GSNO than A^{434}. One explanation may be that a negatively-charged Asp can favor the thiol form of C^{433} and/or repel an approaching GSNO molecule better than a small hydrophobic amino acid. GSHsite predicted that the BAM1-D430H mutant would be the most sensitive to GSNO, but it was also predicted that BAM1-A434S would be less sensitive to GSNO than the BAM1 WT. This indicates that the primary structure alone, which is what GSHsite uses, is not always enough to predict glutathionylation sensitivity. Some residues that are close to C^{433} in the tertiary structure but not close in the primary structure may also influence the sensitivity of C^{433} in BAM1 and BAM3 to GSNO, but GSHsite only analyzes the 10 amino acids before and after cysteines in the primary structure. However, in the homology models of BAM1 and BAM3, there were no differences found in the tertiary structure that could not be found within the 10 amino acids before and after C^{433}.

The underlying causes of glutathionylation of C^{433} and of Cys residues in general are still not entirely understood. Our unique system in which we can make mutations around C^{433} in BAM1 and BAM3 without destroying enzyme activity completely can still be exploited to test the effects of specific amino acids on the susceptibility of C^{433} to glutathionylation. Further analysis of the BAM3 single mutants can give us a better idea of how H^{430}, N^{432}, and S^{434} affect the sensitivity of C^{433}. In addition, positions that do not appear to be important in the susceptibility of C^{433} to glutathionylation may work together to make BAM3 sensitive and BAM1 insensitive to GSNO. Therefore, double and triple mutants with two and three amino acid substitutions could reveal synergistic effects among these positions. Finally, computational analysis could be improved by crystallizing BAM1 and BAM3 to obtain accurate structures of

these enzymes. X-Ray crystallography could provide exact orientations of the amino acid residues surrounding C^{433}, distances between potential hydrogen-bonding groups, and accurate solvent exposure calculations. Reliable predictions from crystal structures can be tested with mutants to further uncover the biochemical reasons for the difference in sensitivity of C^{433} to glutathionylation in BAM1 and BAM3.

Literature Cited

Corpas F.J., Alche J.D., Barroso, J.B. 2013. Current overview of S-nitrosoglutathione (GSNO) in higher plants. *Frontiers in Plant Science*. 4: 1-3.

Dalle-Donne I., Rossi R., Giustarini D., Colombo R., Milzani A. 2007. S-glutathionylation in protein redox regulation. *Free Radical Biology and Medicine*. 43: 883-898.

Ferrer-Sueta G., Manta B., Botti H., Radi R., Trujillo M., and Denicola A. 2011. Factors affecting protein thiol reactivity and specificity in peroxide reduction. *Chem. Res. Toxicol*. 24: 434-450.

Fulton D.C, Stettler M., Mettler T, Vaughan C.K., Li J., Francisco P., Gil M., Reinhold H., Eicke S., Messerli G., Dorken G., Halliday K., Smith A.M., Smith S.M., Zeeman S.C. 2008. β-AMYLASE4, a noncatalytic protein required for starch breakdown, acts upstream of three active b-amylases in Arabidopsis chloroplasts. *Plant Cell*. 20: 1040-1058.

Gallogly M.M, Mieyal J.J. 2007. Mechanisms of reversible protein glutathionylation in redox signaling and oxidative stress. *Current Opinion in Pharmacology*. 7: 381-391.

Gayatri G., Agurla S., Raghavendra A.S. 2013. Nitric oxide in guard cells as an important secondary messenger during stomatal closure. *Frontiers in Plant Science*. 4: 425.

Ghezzi P., Casagrande S., Massignan T., Basso M., Bellachio E., Mollica L., Biasini E., Tonelli R., Ebernini I., Gianazza E., Dai W., Fratelli M., Salmona M., Sherry B., Bonetto V. 2006. Redox regulation of cyclophilin A by glutathionylation. *Proteomics*. 6: 817-825.

Graf A., Schlereth A., Sitt M., Smith A.M. 2010. Circadian control of carbohydrate availability for growth in Arabidopsis plants at night. *P Natl Acad Sci USA.* 107: 9458-9463.

Grek C.L., Zhang J., Manevich Y., Townsend D.M., Tew K.D. 2013. Causes and consequences of cysteine S-glutathionylation. *J. Biol. Chem.* 288: 26497-26504.

Horrer D., Flutsch S., Pazmino D., Matthews J., Thalmann M., Nigro A., Leonhardt N., Lawson T., Santelia D. 2016. Blue light induces a distinct starch degradation pathway in guard cells for stomatal opening. *Current Biology*. 26: 362-370.

Hye-Won S., George S.C. 2001. Microscopic modeling of NO and *S*-nitrosoglutathione kinetics and transport in human airways. *Journal of Applied Physiology*. 90: 777-788.

Kang Y.N., Adachi M., Utstumi S., Mikami B. 2004. The roles of Glu186 and Glu380 in the catalytic reaction of soybean beta-Amylase. *J. Mol. Biol.* 339: 1129-1140.

Kaplan F., Guy C.L. 2004. β-Amylase induction and the protective role of maltose during temperature shock. *Plant Physiology.* 135: 1674–1684.

Krieger E., Vriend G. 2014. YASARA View - molecular graphics for all devices - from smartphones to workstations, *Bioinformatics* 30: 2981-2982.

Leterrier M., Chaki M., Hiraki M., Valderrama R., Palma J.M., Barroso J.B., Corpas F.J. Function of S-nitrosoglutathione reductase (GSNOR) in plant development and under biotic/abiotic stress. *Plant Signal Behav.* 6: 789-793.

Li J., Francisco P., Zhou W., Edner C., Steup M., Ritte G., Bond C.S., Smitch S.M. 2009. Catalytically-inactive β-amylase BAM4 required for starch breakdown in Arabidopsis leaves is a starch binding-protein. *Arch Biochem Biophys.* 489: 92-98.

Lum H.K., Lee C.H., Butt Y.K.C., Lo S.C.L. 2005. Sodium nitroprusside affects the level of photosynthetic enzymes and glucose metabolism in *Phaseolus aureus* (mung bean). *Nitric Oxide*. 12: 220-230.

Madzelan P., Labunska T., Wilson M.A. 2012. Influence of peptide dipoles and hydrogen bonds on reactive cysteine pKa values in fission yeast DJ-1. *FEBS Journal*. 279: 4111-4120.

Marino S.M., Gladyshev V.N. 2009. A structure-based approach for detection of thiol oxidoreductases and their catalytic redox-active cysteine residues. *PLoS Comput. Biol.* 5.

Miranda J.L. 2003. Position-dependent interactions between cysteine residues and the helix dipole. *Protein Science*. 12: 73-81.

Monroe J.D., Storm A.S., Badley E.M., Lehman M.D., Platt S.M., Saunders L.K., Schmitz J.M., Torres C.E. 2014. β-Amylase1 and β-Amylase3 Are Plastidic Starch Hydrolases in Arabidopsis That Seem to Be Adapted for Different Thermal, pH, and Stress Conditions. *Plant Physiology*. 166: 1748-1763.

Nelson N. 1944. A photometric adaptation of the Somogyi method for the determination of glucose. *J. Biol. Chem.* 153: 375-380.

Niittyla T., Messerli G., Trevisan M., Chen J., Smith A.M., Zeeman S.C. 2004 A previously unknown maltose transporter essential for starch degradation in leaves. *Science*. 303: 87-89.

Popov D. 2014. Protein S-glutathionylation: from current basics to targeted modifications. *Arch. Physiol. Biochem.* 12: 123-130.

Reinhold H., Soyk S., Simkova K., Hostettler C., Marafino J., Mainiero S., Vaughan C.K., Monroe J.D., Zeeman S.C. 2011. β-amylase-like proteins function as transcription factors in Arabidopsis, controlling shoot growth and development. *Plant Cell.* 23: 1391-1403.

Roos G., Foloppe N., Messens J. 2013 Understanding the pK(a) of redox cysteines: the key role of hydrogen bonding. *Antioxid Redox Sign*. 18: 94-127.

Roy A., Kucukural A., Zhang Y. 2010. I-TASSER: a unified platform for automated protein structure and function prediction. *Nature Protocols*. 5: 725-738.

Santelia D., Trost P., Sparla F. 2015. New insights into redox control of starch degradation. *Current Opinion in Plant Biology*. 25: 1-9.

Shekhter T., Metanis N., Dawson P.E., Keinan E. 2010. A residue outside the active site CXXC motif regulates the catalytic efficiency of glutaredoxin 3. *Mol. BioSyst.* 6: 241-248.

Sievers F., Wilm A., Dineen D., Gibson T.J., Karplus K., Li W., Lopez R., McWilliam H., Remmert M., Soding J., Thompson J.D., Higgins D.G. 2011. Fast, scalable generation of high-quality protein multiple sequence alignments using Clustal Omega. *Mol. Syst. Biol.* 7: 539.

Smith A.M., Stitt M. 2007. Coordination of carbon supply and plant growth. *Plant Cell Environ* 30: 1126-1149.

Wang Q., Monroe J., Sjolund R.D. 1995. Identification and characterization of a phloem specific β−amylase. *Plant Physiology.* 109: 743–750.

Yang J., Yan R., Roy A., Xu D., Poisson J., Zhang Y. 2015. The I-TASSER suite: protein and function. *Nature Methods*. 12: 7-8.

Zaffagnini M., Fermani S., Calvaresi M., Orru R., Iommarini L., Sparla F., Falini G., Bottoni A., Trost P. 2016. Tuning cysteine reactivity and sulfenic acid stability by protein microenvironment in glyceraldehyde-3-phosphate dehydrogenase of Arabidopsis thaliana. *Antioxid. Redox. Signal.* 24: 502-517.

Zeeman S.C., Kossmann J., Smith A.M. 2010. Starch: its metabolism, evolution, and biotechnological modification in plants. *Annual Review of Plant Biology*. 61: 209-234.

Zeeman S.C., Smith S.M. Smith A.M. 2004. The breakdown of starch in leaves. *New Phytologist*. 163: 247-261.

Zeeman S.C., Smith S.M., Smith A.M. 2007. The diurnal metabolism of leaf starch. *Biochemical Society*. 401:13-28.

Zhang Y. 2008. I-TASSER server for protein 3D structure prediction. *BMC Bioinformatics*. 9: 40.